CO_2 capture in combined cycles with air-blown gasification of pre-dried high-moisture lignite

Antonio Giuffrida[a], Stefania Moioli[b] and Laura A. Pellegrini[b]

[a] Politecnico di Milano - Dipartimento di Energia, Milano, Italy, antonio.giuffrida@polimi.it
[b] Politecnico di Milano - Dipartimento di Chimica, Materiali e Ingegneria Chimica "G. Natta", Milano, Italy, stefania.moioli@polimi.it, laura.pellegrini@polimi.it

Abstract:

This paper deals with the energy impact of pre-combustion CO_2 capture in air-blown IGCC plants when gasifying pre-dried high-moisture lignite.
An original in-house code, integrated with Aspen Plus®, was used to carry out the thermodynamic IGCC assessment, which points out that a significant lignite pre-drying is necessary for higher efficiency. Considering a residual moisture in the pre-dried lignite ranging from 10 to 30 wt%, HHV efficiency presents a decreasing trend, with a maximum value slightly less than 37% for 90% of CO_2 avoided, even though the higher the residual moisture in the pre-dried lignite, the lower the extraction of steam from the bottoming cycle of the IGCC plant for the water-gas shift reaction. However, introducing the specific primary energy consumption for CO_2 avoided (SPECCA) as an index for the energy cost related to CO_2 capture, reductions seem to be possible when gasifying pre-dried lignite with higher residual moisture. In particular, a SPECCA value as low as 2.79 MJ/kg_{CO2} has been calculated for the case with the highest (30 wt%) residual moisture in the lignite. Ultimately, measures for energy saving at the CO_2 capture and storage plant are investigated as well.

Keywords:

Air-blown, coal drying, CO_2 capture, high-moisture lignite, IGCC, SPECCA.

1. Introduction

The integrated gasification combined cycle (IGCC) stands out in the field of the clean coal technologies, due to its excellent environmental features together with its high thermal efficiency. Among other benefits, IGCC plants offer considerable flexibility of fuel supply.

1.1 The air-blown IGCC technology

Coal gasification is the core of an IGCC. Although most of the demonstration projects on large-scale IGCC plants are based on oxygen-blown gasifiers, the air-blown technology should also be considered because of the economic advantage related to the much smaller ASU and the potentially higher IGCC efficiency [1]. A significant activity on air-blown coal gasification has been conducting during the last years by Mitsubishi Heavy Industries (MHI) in Japan, where the 250 MW_{el} demonstration plant in Nakoso was started up in 2007 [2]. Considering both the first results and further technological improvements, MHI declares interesting performance (600 MW_{el} for gross power and 53% for gross LHV efficiency) for short-term commercial power plants [3].

A thermodynamic assessment of an air-blown gasification-based combined cycle was carried out in a previous study [1], based on public information from MHI. After reproducing the mass and energy balance of a large-scale MHI-type air-blown gasifier, a complete IGCC plant was proposed and its performance compared to the one of an IGCC with an oxygen-blown Shell-type gasification system, calculated with coherent assumptions and the same combustion turbine. In particular, a net efficiency resulting 1.5 percentage points higher than the one characterizing the reference oxygen-blown IGCC was calculated. Air-blown IGCC technology has been thoroughly studied in the recent years. Solutions based on hot fuel gas clean-up and an advanced 1500°C-class combustion turbine as topping cycle [4], as well as solutions based on post-combustion CO_2 capture by MEA [5] and

aqueous ammonia [6] scrubbing were assessed from a thermodynamic point of view. Currently, attention is paid to pre-combustion CO_2 capture [7], as reported in the following.

1.2 Novel contribution of this paper

The effective utilization of high-moisture coal like brown coal, lignite and sub-bituminous coal is one of the most important subjects for the world-wide energy benefit [8]. MHI expectation is directed to gasify even lignite [9], based on the relatively low ash melting point and the easier gasification than bituminous coals, thanks to the low ratio between fixed carbon and volatile matter.

The current work follows a recent study dealing with the exploitation of low-rank coals in air-blown IGCC plants [10] and investigates the thermodynamic performance of plants with CO_2 pre-combustion capture when a high-moisture lignite replaces the more common bituminous coal as fuel input. Thus, the work is original in the sense that there are no papers in technical literature focusing on combined cycles based on air-blown gasification of lignite with CO_2 capture. In detail, three levels of pre-drying are considered to in-depth understand the effects of residual moisture content in the lignite. Measures to limit the energy demand by the CO_2 capture plant are investigated as well.

2. Lignite drying

Low-rank coals present high-moisture content, typically 30-60 wt%, resulting in low heating value, low thermal efficiency in combustion and high transportation costs. When high-moisture coals are burned in boilers, about 7-10% of the fuel input is used to evaporate the moisture [11], reflecting on (i) higher fuel flow, (ii) higher flue gas flow, (iii) higher power consumption, (iv) lower plant efficiency and (v) higher maintenance costs. Also, the moisture causes a reduction in the friability of the coal, making it difficult to control blending operations and worsening the quality of grinding and the pneumatic transport of the pulverized coal.

After decades of research and development, several technologies for low-rank coal drying and dewatering are now available, such as rotary dryers, fluidized bed dryers, microwave dryers, screw conveyor dryers, etc. [12]. Although the most commonly used dryers for drying brown coal are the rotary-type ones, fluidized bed drying with superheated steam is a very interesting option. The concept of superheated steam drying in a fluidized bed with internal heat exchangers has been refined into the WTA (German acronym for "fluidized bed dryer with integrated waste heat recovery") process proposed by RWE Power AG. As schematized in Fig. 1, after being milled and pre-heated in a heat exchanger by condensed water from the drying process of the previous charge, the raw brown coal enters the dryer, where it is fluidized under the influence of lightly superheated steam. The heat necessary for moisture heating and evaporation is mainly provided by pressurized steam from the previous charge drying in a heat exchanger. The steam used for fluidization also contributes to the evaporation of coal moisture. After being cleaned, the evaporated moisture is compressed to the dryer, with a small part used for fluidization. As regards the capacity of a WTA drying pilot plant, 26 t/h of moisture may be removed from 53 t/h of raw brown coal [13], so the WTA process has been presented as a solution for low-rank coal drying by Shell [14]. More

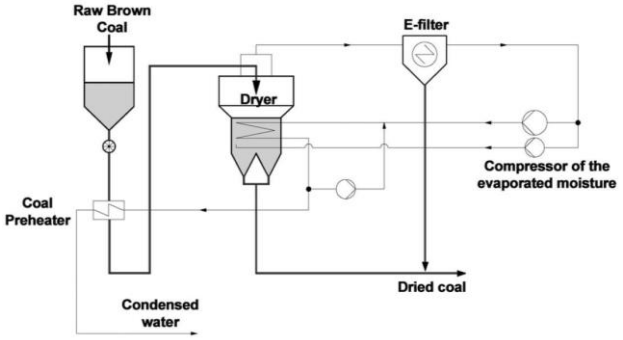

Fig. 1. Schematic of a brown coal drying system based on the WTA process (adapted from [13]).

recently, similar solutions for lignite drying have been proposed by Aziz et al. [15]: based on self-heat recuperation, the energy involved in the drying process is always recirculated and reutilized, with a very low energy consumption, apart from the heat loss due to blowdown requirements.

3. Lignite-fired IGCC with CO_2 capture

The air-blown IGCC plant investigated in this work is based on the one early reported in [16] and further revised. Each IGCC plant consists of two gasification trains and two combustion turbines with two heat recovery steam generators, which share the same steam turbine.

As schematized in Fig. 2, the high-moisture lignite (1) enters a WTA unit, whose operation has been presented before. After drying and moisture removal, the pre-dried lignite (2) is loaded by means of a fraction of the CO_2 captured in the AGR station and recycled back (3), so that the air separation unit necessary in the plant with no CO_2 capture to deliver enough N_2 for coal loading is not employed here. The air entering the two-stage gasification system is extracted from the CT compressor outlet, partly cooled down to about 350°C by producing HP steam and finally boosted to the bottoming stage of the gasification system. This air stream must be sufficient to burn the pulverized coal and the recycled char at high temperature (1900°C), so that the coal ash is discharged as molten slag. The bottoming stage supplies sufficient heat to the topping one where the high-temperature coal-derived gas is chemically quenched and experiences a temperature drop of about 700°C. The raw syngas exiting the gasifier (9) is cooled (i) down to about 350°C (11) by producing HP super-heated steam and (ii) down to 150°C (12), before scrubbing, by economization of HP water. A sour WGS station, with two reactors and two heat exchangers, necessary to both pre-heat the syngas and to recover the heat of the exothermic water-gas shift reaction, is present after the scrubber. In detail, the syngas exiting the scrubber is firstly pre-heated in a regenerative gas-gas heat exchanger and then mixed with MP steam (13), extracted from the steam turbine, before entering the first WGS reactor. The shifted syngas exiting this WGS reactor at temperature slightly less than 500°C is firstly cooled down to about 350°C by producing HP steam and used as the hot stream in the regenerative gas-gas heat exchanger to pre-heat the syngas exiting the scrubber. Then, the shifted syngas at 210°C (14) enters another WGS reactor to complete the CO to CO_2 conversion: 95.3% of the total carbon in the shifted syngas is finally present as CO_2. The shifted syngas exiting the second WGS reactor is then cooled down to 150°C (16) by heating the H_2-rich stream fuelling the combustion turbine. It is further cooled down to near-ambient temperature for acid gas removal, releasing heat for pre-heating the clean syngas from the AGR station and water for the steam cycle and for syngas scrubbing. H_2S and CO_2 are selectively removed by means of a MDEA-based process (as described in detail in the next section) and sent to a Claus unit and to permanent storage respectively.

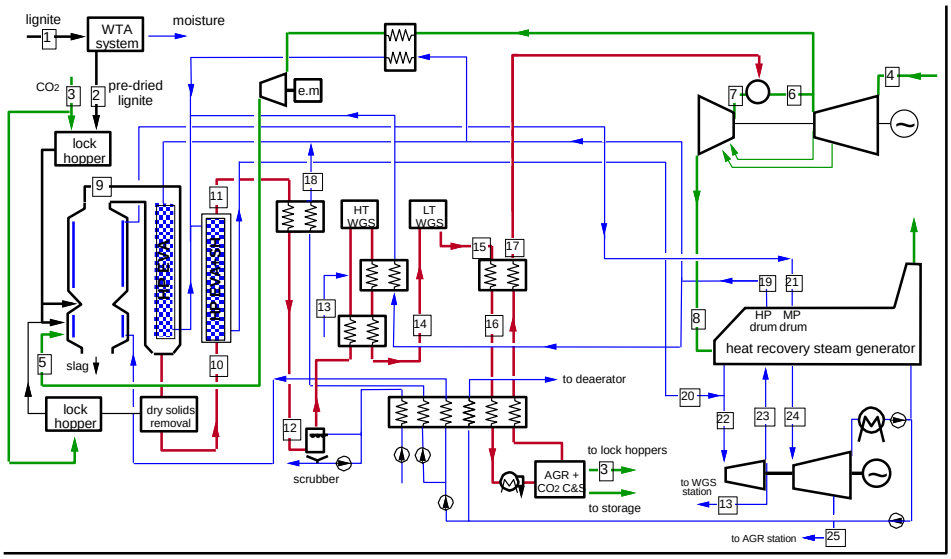

Fig. 2. Schematic of the lignite-fired IGCC with CO_2 capture.

The H_2-rich stream exiting the AGR station is heated up to about 230°C (17) in a regenerative heat exchanger before fuelling the combustion turbine of the IGCC plant. The CT exhaust heat is recovered in a two pressure level (36 and 144 bar) steam cycle with reheat, along with the heat from syngas cooling, which is larger compared to the case with no CO_2 capture [10] owing to (i) the larger syngas flow rate, (ii) the exothermic water-gas shift reaction and (iii) the increased flow rate due to the injection of steam upstream of the WGS station. Another slight heat contribution to the steam cycle comes from the gasification air cooling before its boosting.

4. Simulation environments

Mass and energy balances of the IGCC plants were carried out with the code GS [17], which is an in-house simulation tool originally designed to calculate gas-steam cycles as well as complex energy conversion systems. It has proved to yield highly accurate results in estimating the performance of combustion turbines and combined cycles [18] and has been successfully used to simulate a variety of power plant configurations, including gasification processes [19] and other chemical reactors [20]. The main features of the code include: (i) the capability of reproducing even complex plant schemes by assembling basic modules, such as turbine, compressor, heat exchanger, etc., (ii) the use of built-in correlations for efficiency prediction of turbomachinery, as a function of their operating conditions, (iii) the use of built-in correlations for gas turbine cooling flows, (iv) the capability of calculating chemical equilibrium by Gibbs free energy minimization.

The acid gas removal units were simulated by using the commercial software ASPEN Plus®, chosen because of its great flexibility and customized in order to obtain a reliable tool for simulation. For a correct design of the process, both thermodynamics and mass transfer with reactions should be properly represented. The chemical reactions occurring in the liquid phase involve the presence of ionic species, making the system strongly non-ideal. Vapor-liquid equilibrium was described by means of the Electrolyte-NRTL model (by default implemented in ASPEN Plus®) with *ad hoc* parameters [21-22], regressed on the basis of experimental data. A rate-based approach has been used for the modelling of the absorption and regeneration columns, considering the real phenomena of diffusion with reaction occurring on each tray. ASPEN Plus® by default uses film theory, which in literature [23] is considered not appropriate for the description of these systems. Another model, based on the Eddy Diffusivity theory and on the Interfacial Pseudo First Order assumption, can be successfully used to model amine scrubbing systems [24-25] and was introduced by linking an external subroutine to the commercial simulator [26]. Finally, the Soave-Redlich-Kwong equation of state was used for CO_2 compression simulation in ASPEN Plus® [16].

The simulation of the AGR station was performed with the aim of designing a scheme for a selective absorption, in order to satisfy the specifications for the H_2S content in the CO_2-rich stream to storage [27]. Two sequential processes should be considered: the first for H_2S absorption (along with a little amount of CO_2) and the second for CO_2 absorption (no less than 95% of the CO_2 in the coal-derived gas entering the AGR station). Figs 3 and 4 show the schematic of these purification plants, as modelled in the ASPEN Plus® environment.

As shown in Fig. 3, the stream sent to the AGR station is mixed with two compressed recycle streams, RICIRC and CLAUSREC, before entering the first absorption column for the selective removal of H_2S. The solvent, exiting the bottom of the absorption column and rich in H_2S is regenerated by flash and distillation. FLASH helps in separating part of the absorbed CO_2 by simply lowering the pressure down to 1 bar, with no energy supply[1]. A heat exchanger (CROSS) is present to recover most of the heat supplied at the reboiler of the distillation column and to simultaneously feed the rich amine solution to REGH2S at higher temperature. The gaseous stream

[1] In particular, the amount of CO_2 in FLASHVAP is very high (85-90% on a molar basis) compared to the one of H_2S, which largely remains in the liquid phase and exits in H2SPROD in higher concentration than the one that would be found without the flash unit. FLASHVAP also contains the absorbed H_2 (N_2 and water also), which is not lost in this unit, but recovered and mixed to the H_2S-free syngas sent to the CO_2 removal unit.

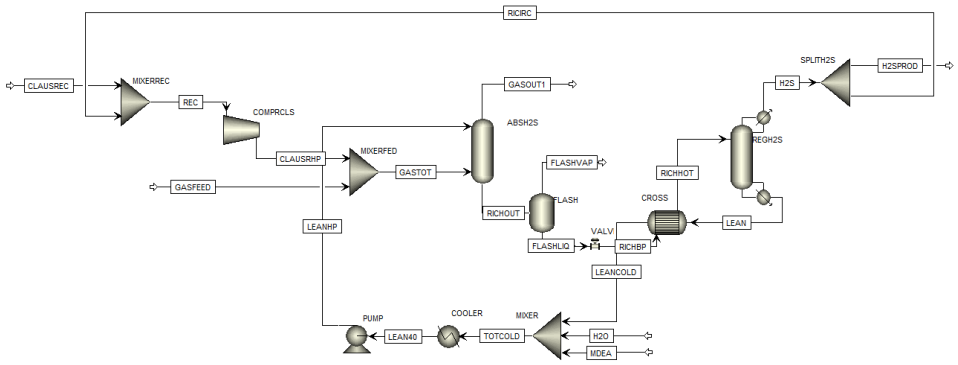

Fig. 3. Screenshot of the H_2S removal unit in ASPEN Plus®.

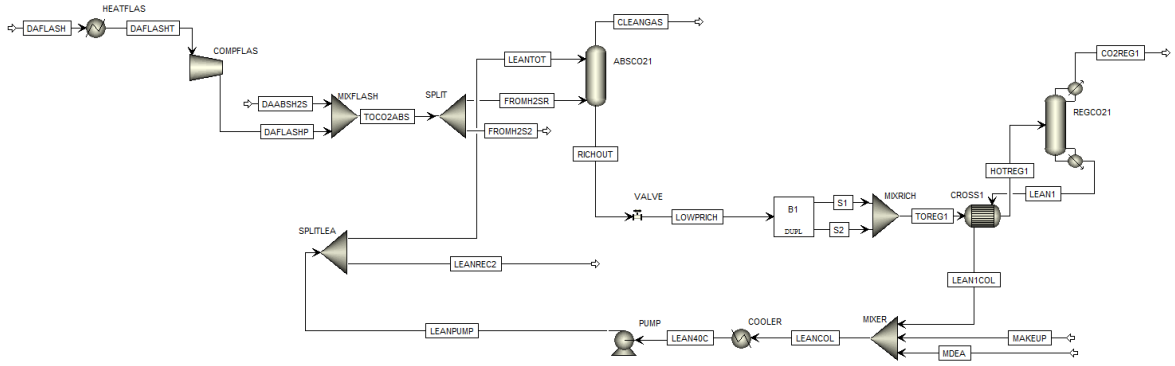

Fig. 4. Screenshot of the CO_2 removal unit in ASPEN Plus®.

from the regeneration column is split into two streams: H2SPROD to the Claus unit[2] and RICIRC[3] to the absorption section. The gaseous streams exiting the absorption column (GASOUT1) and the flash vessel (FLASHVAP) are sent to the next plant, as DAFLASH and DAABSH2S in Fig. 4.

The CO_2 removal unit in Fig. 4 consists of two parallel absorption columns with one regeneration column. Two absorption columns were considered to perform the desired CO_2 removal for the investigated cases, characterized with not so high driving force and high amount of carbon dioxide, as syngas pressure at AGR inlet is equal to 24.1 bar and CO_2 concentration is about 27 vol%[4]. Thus, both the gaseous feed (TOCO2ABS) and the liquid solvent (LEANPUMP) are split into two identical streams before entering the column ABSCO21 (or ABSCO22, not shown in Fig. 4) for CO_2 absorption. Both the rich amine solutions exiting ABSCO21 and ABSCO22 are sent to the column REGCO21 for regeneration. The lean amine solution, with a low CO_2 content (about $2.7 \cdot 10^{-3}$ on a molar basis) and a very low H_2S content (about 10^{-5} on a molar basis), is pumped to the two absorption columns through a heat exchanger (CROSS1) for pre-heating the rich amine solution. As shown on the left in Fig. 5, the amine circulation rate was chosen in order to satisfy the specification of CO_2 removal. CO2REG1 is finally sent to an intercooled compression station and further split into two streams: one recycled back to the gasification station for pre-dried lignite loading and another pumped to permanent storage.

---

[2] CLAUSREC is a stream containing part of the H_2S (4%) and the CO_2 (100%) in H2SPROD.

[3] Stream RICIRC is fundamental in order to guarantee a content of H_2S in the gas flowing out of the H_2S stripper acceptable for feeding a Claus plant. By recycling part of the gaseous stream from the stripper to the absorption section, the H_2S to CO_2 ratio varies and the H_2S partial pressure of stream GASTOT is higher, causing an increase in the amount of H_2S absorbed into the amine solution.

[4] On the other hand, preliminary simulations showed that simply increasing the amount of the circulating amine solvent is not a favourable solution.

The main assumptions for the IGCC calculations in both the GS and ASPEN Plus® platforms are reported in the Appendix.

5. Results and discussion

The main results of this work are detailed in the next sub-sections. After some considerations on the properties of the lignite and on the energy consumptions for drying, basic results of IGCC calculations are reported, along with the main results of a parametric analysis oriented to possible reductions in energy demand by the CO_2 capture process.

5.1 High-moisture lignite and its pre-drying

The fuel considered in this work is a high-moisture Australian lignite, chosen based on the data reported by Aziz et al. [15] for the relationship between the equilibrium water content of the wet solid and the relative vapour pressure. As a matter of fact, the operation conditions of the drying process strongly depend on solid-water interactions. Table 1 details the ultimate analyses of the lignite, as received as well as after three pre-drying levels. Paying attention to both the heating values, it is possible to realize the difference between HHV and LHV, obviously greater for higher moisture content. In detail, starting from 1 kg of as-received lignite, it is necessary to remove 0.5 kg of water for case L30. On the other hand, 0.563 kg and 0.611 kg of water have to be removed for cases L20 and L10, respectively. The specific compression work in a WTA-type drying system is reported on the right in Fig. 5, based on previous calculations [10]. According to the relationship between the equilibrium water content of the wet solid and the relative vapour pressure, the specific compression work related to lignite drying was calculated. In particular, an energy balance was applied to the open system schematized in Fig. 1, where it is possible to count one raw lignite input,

Table 1. Characteristics of the lignite, as received and after drying

	Lignite AR	*L10*	*L20*	*L30*
Ultimate analysis, wt%				
Carbon	23.35	60.03	53.36	46.69
Hydrogen	0.11	0.27	0.24	0.21
Nitrogen	0.21	0.54	0.48	0.42
Sulfur	1.65	4.23	3.76	3.29
Oxygen	9.10	23.4	20.8	18.2
Ash	0.60	1.53	1.36	1.19
Moisture	65.0	10	20	30
HHV, MJ/kg	9.07	23.31	20.72	18.13
LHV, MJ/kg	7.12	22.14	19.41	16.68

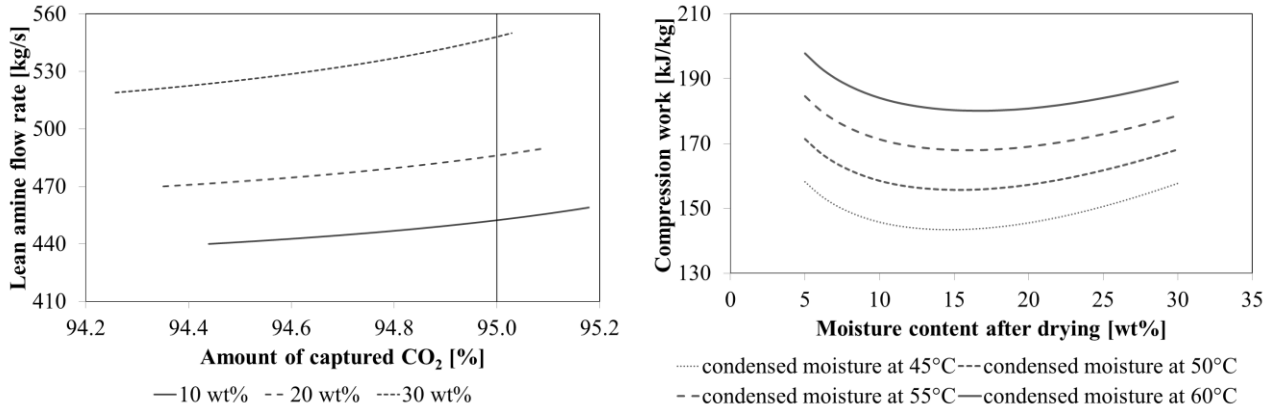

Fig. 5. Amine flow rate as a function of the CO_2 removal rate for three cases of shifted syngas from pre-dried lignite with different residual moisture contents (on the left); compression duty for lignite drying as a function of the residual moisture content at different temperatures of the condensed water exiting the drying system (on the right).

along with the power demand for vapor compression, and two outputs, i.e. the dried lignite (with a residual moisture content) and the condensed moisture removed from the input lignite, exiting firstly the drier and finally the lignite pre-heater. No heat losses were considered from the drying system to the surroundings, for the sake of simplicity. Values reported on the right in Fig. 5, where the temperature of the condensed moisture exiting the drying system is a key-parameter, are consistent with calculations by other authors [13]. In particular, as regards the results detailed in the following, the condensed moisture is supposed to leave the coal pre-heater at 60°C.

5.2 IGCC calculations

The results of the IGCC calculations are reported in Table 2 and discussed with reference to power balances and main stream characteristics. In detail, the size of the IGCC plant depends on the CT technology at the topping cycle with particular reference to the assumed mass flow rate (665 kg/s) exiting the CT expander (see Table A.2), resulting in three IGCC sizes.

Paying first attention to the pre-dried lignite to carbon-free syngas conversion before fuelling the combustion turbine, syngas quality degrades if compared to the cases with no CO_2 capture (see Table A.4). The water-gas shift reactions prior to the acid gas removal are responsible for such a result. Moreover, the higher the amount of moisture in the lignite the lower the syngas quality, so more fuel will be necessary at the CT inlet for the specified firing temperature.

Table 2. Power balances and main stream details for the IGCC plants with CO_2 capture

	L10	*L20*	*L30*
Power balance for one gasification train, MW_{el}			
Combustion turbine	277.6	276.2	274.1
Steam turbine	259.8	286.3	324.7
Steam cycle and condenser pumps	5.9	6.4	6.9
Vapour compression for coal drying	23.7	24.6	27.7
Air booster compressor	24.6	27.5	31.8
CO_2 compression	38.3	41.0	44.9
IGCC auxiliaries	14.0	14.9	16.1
Overall results			
Cold gas efficiency, %	66.9	64.7	61.7
Net electric power, MW_{el}	861.7	896.6	942.6
Net electric HHV efficiency, %	36.89	36.39	35.49
Net electric LHV_{AR} efficiency, %	46.98	46.34	45.19
Net electric LHV_{AD} efficiency, %	38.84	38.84	38.58
Specific emissions, kg_{CO2}/MWh	99.3	102.1	106.2
SPECCA, MJ/kg_{CO2}	3.13	3.00	2.79
Lignite to each drying system, kg/s	128.8	135.9	146.5
Air at each CT compressor inlet, kg/s	686.4	690.2	696.0
Coal-derived gas exiting each gasifier, kg/s	217.4	247.9	293.2
Fuel gas to each CT combustor, kg/s	133.8	148.7	170.9
Fuel gas LHV, MJ/kg	5.55	5.02	4.41
HP steam entering the turbine, kg/s	421.3	445.5	480.0
Heat rejected at the condenser, MW	520.1	584.6	677.8

Three electric efficiencies have been calculated, namely the HHV efficiency:

$$\eta_{HHV} = \frac{\text{IGCC net power}}{\dot{m}_{\text{lignite AR}} \cdot HHV_{\text{lignite AR}}} = \frac{\text{IGCC net power}}{\dot{m}_{\text{lignite AD}} \cdot HHV_{\text{lignite AD}}} \quad (1)$$

as well as two LHV efficiencies based on both the as-received and pre-dried lignites. Referring to the heat input based on the LHV of the as-received lignite, higher efficiency values than the ones calculated for IGCCs fired with bituminous coals [1] can be appreciated and justified according to the actual difference between HHV and LHV reported in Table 1. However, focusing on the LHV efficiency calculated in compliance with the pre-dried lignite, the values do not present a clear trend, with a slight reduction for case L30 only, even though the higher the residual moisture in the

lignite the lower this figure of merit in IGCCs with no CO_2 capture (in Table A.4). If reference to the HHV efficiency as a figure of merit is made in order to avoid misleading conclusions, a clear trend with continuous reductions for higher residual moisture contents can be appreciated.

When dealing with decarbonized power production, a measure of the energy cost related to CO_2 capture must be introduced along with IGCC efficiency, so the specific primary energy consumption for CO_2 avoided (SPECCA) defined as:

$$\mathrm{SPECCA} = \frac{\mathrm{HR} - \mathrm{HR_{ref}}}{\mathrm{ER_{ref}} - \mathrm{ER}} = \frac{3600 \cdot \left(\frac{1}{\eta} - \frac{1}{\eta_{\mathrm{ref}}}\right)}{\mathrm{ER_{ref}} - \mathrm{ER}} \tag{2}$$

has been calculated. The reference IGCC plant with no CO_2 capture and fired with pre-dried lignite at the same residual moisture content is considered for SPECCA calculations, as reported in Table A.4. On the whole, SPECCA values are slightly lower than the ones calculated for IGCC plants fired with a bituminous coal [7]. In particular, the lowest SPECCA for case L30 can be justified by considering (i) the lower efficiency of the corresponding power plant with no CO_2 capture [10] and (ii) the lower steam extraction from the IGCC bottoming cycle to the WGS station (thanks to the higher residual moisture in the lignite), which reflects on a reduced efficiency penalty due to CO_2 capture.

Based on the same combustion turbine, with really slight variations in power output for the three cases in Table 2, the trend of the overall net power output is opposite to the ones for HHV efficiency and SPECCA. Nevertheless, the higher residual moisture in the lignite brings about larger components in the gasification station as well as larger steam turbine and condenser. Mass flow rates for the main streams in Fig. 2 are reported in Table 2 for the sake of completeness: they give an idea of the size of the main IGCC components.

5.3 Parametric analysis

Without significantly modifying the lay-out of the CO_2 removal unit, further simulations have been run to investigate possible energy savings. In particular, the pinch point ΔT at the regenerative heat exchanger (CROSS1 in Fig. 4) was reduced from 10 to 5°C and the pressure at the distillation column (REGCO21 in Fig. 4) was raised from 1 to 2 and 3 bar. Variations of these two parameters directly affect the heat duty for CO_2 stripping, whereas the regeneration pressure reflects on CO_2 compression work. Moreover, increasing the regeneration pressure causes different H_2S-to-CO_2 ratios at vapour-liquid equilibrium conditions and thus lower loadings in the lean solvent, whose circulation rate (required for a fixed CO_2 removal) can be reduced.

Although the input feedstock to the IGCC plant does not vary, new sets of results have been analysed for each pre-dried lignite reported in Table 1. Variations in steam turbine power output, as

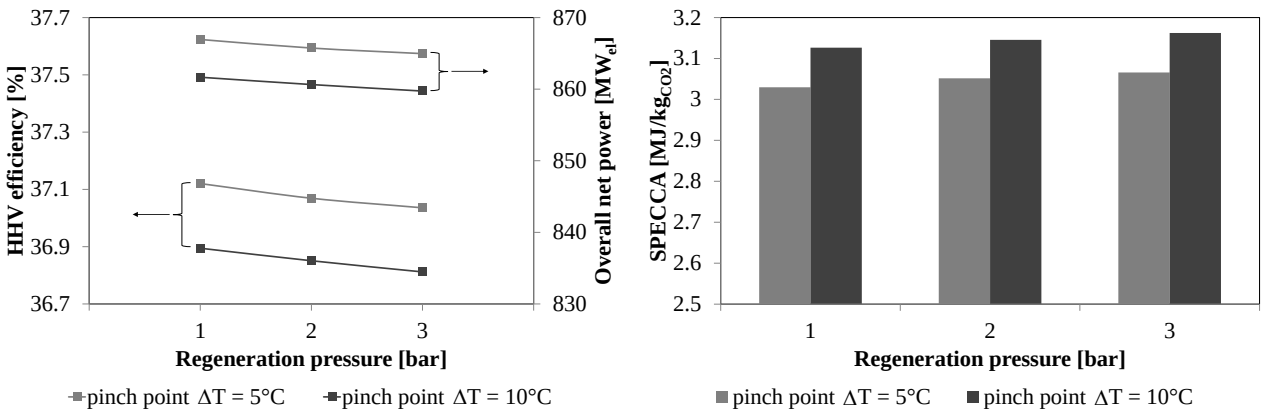

Fig. 6. HHV efficiency and net power (on the left) and SPECCA (on the right) for the case of lignite with residual moisture of 10 wt%.

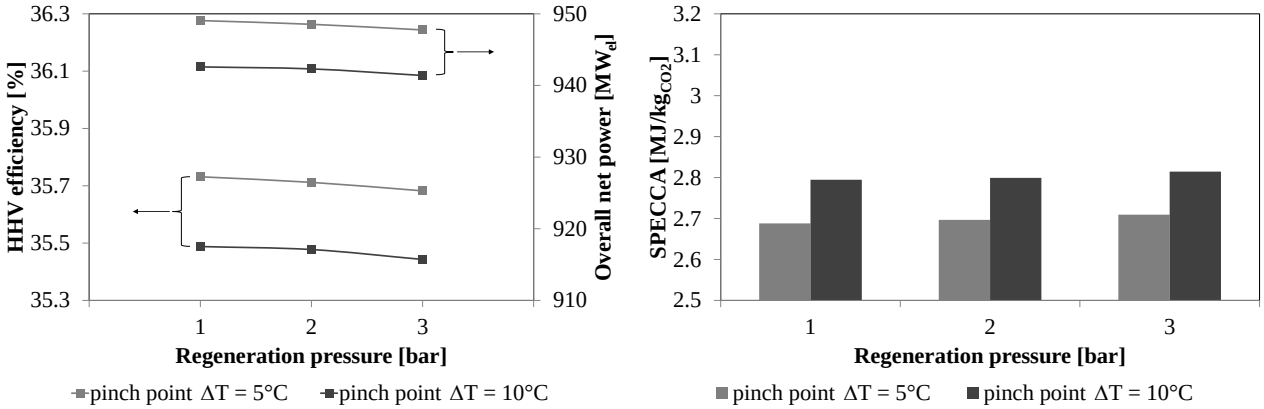

Fig. 7. HHV efficiency and net power (on the left) and SPECCA (on the right) for the case of lignite with residual moisture of 30 wt%.

well as energy consumptions for AGR auxiliaries and CO_2 compression, have been calculated and new results are reported in Figs 6 and 7, limited to two cases for the sake of conciseness (results for case L20 are intermediate between these two cases). As plausible, reducing the pinch point ΔT at the regenerative heat exchanger, thanks to an advanced technology, brings about slight increases in IGCC efficiency and net power, i.e. slight reductions in both the CO_2 emission rate and the SPECCA. On the other hand, raising the regeneration pressure seems to result in slight reductions in efficiency, power output as well as SPECCA.

6. Conclusions

An original work focusing on air-blown IGCC plants fired with high-moisture lignite and including CO_2 capture has been presented.

HHV efficiency and SPECCA have been used as figures of merit for the IGCC plants. Considering a residual moisture in the pre-dried lignite ranging from 10 to 30 wt%, SPECCA reductions seem to be possible when gasifying pre-dried lignite with higher residual moisture, with a value as low as 2.79 MJ/kg_{CO2} for the case with the highest (30 wt%) residual moisture. Nevertheless, HHV efficiency reduces from a maximum value slightly less than 37% for 90% of CO_2 avoided in case of high residual moisture, even though the higher the residual moisture in the pre-dried lignite, the lower the extraction of steam from the bottoming cycle of the IGCC plant for the water-gas shift reaction. Moreover, the higher the residual moisture in the pre-dried lignite, the larger the size of the IGCC components, with the exception of the combustion turbine which is the same for all the investigated cases.

As a measure to limit the energy demand by the CO_2 capture plant, the adopted heat exchanger technology should be as advanced as possible, whereas raising the operation pressure at the column where CO_2 stripping occurs does not offer any energy advantage.

Appendix A

The following tables detail the main assumptions for IGCC calculations.

Table A.1. Main assumptions for gasification station calculations[5]

Gasification pressure, bar	30.4
Temperature/pressure of gasifying air, °C/bar	495/35.8
Air booster polytropic efficiency, %	90.5
Steam to CO ratio at 1st WGS reactor	1.5
Pressure loss in WGS reactors, %	3
Syngas temperature at 2nd WGS inlet, °C	210

[5] These data are additional to the details reported in [1].

Table A.2. Main assumptions for power cycle calculations[6]

Combustion turbine	
Air pressure loss, %	1
Compressor pressure ratio	18.1
Compressor polytropic efficiency, %	92.25
Compressor leakage, % of the inlet flow	0.75
Fuel valve pressure loss, bar	5
Cooled/Uncooled turbine stage isentropic efficiency, %	91.5/92.5
Turbine inlet temperature, °C	1360
Heat loss at combustor, % of fuel LHV	0.9
Mass flow rate at CT outlet, kg/s	665
CT auxiliaries, % of gross power	0.35
Turbine/compressor mechanical efficiency, %	99.865
Electric generator efficiency, %	98.7
Heat recovery steam cycle	
Pressure loss at the gas side of the heat recovery steam generator, kPa	3
Heat loss, % of transferred heat	0.7
HP/MP level, bar	144/36
Maximum live steam temperature, °C	565
Minimum pinch point ΔT, °C	10
Subcooling ΔT, °C	5
Minimum stack temperature, °C	115
Pressure losses in HP/MP economizers, bar	16/25
Pressure loss in superheaters, %	8
Condensing pressure, kPa	4
Power for heat rejection, MJ_{el}/MJ_{th}	0.01
Pumps hydraulic efficiency, %	80
Turbine mechanical efficiency, %	99.5
Electric generator efficiency, %	98.7

Table A.3. Main assumptions for AGR and CO_2 compression calculations[7]

H_2S removal	
Number of trains	2
Number of absorption/ regeneration columns per train	1/1
Absorber real trays	12
MDEA concentration in the aqueous solution, wt%	10
H_2S content in the CO_2-rich stream to storage, ppm	≤ 200
CO_2 removal	
Number of trains	2
Number of absorption/ regeneration columns per train	2/1
Absorber real trays	51
MDEA concentration in the aqueous solution, wt%	50
Lean/rich solution CO_2 loading	0.02/0.76
Reboiler pressure, bar	1.1
Regeneration column real stages	8
Pinch point ΔT in the recuperative heat exchanger, °C	10
Overall absorbed CO_2, %	95
CO_2 compression	
Number of adiabatic compression stages	4/5
IC compressor isentropic/mechanical-electric efficiency, %	85/94
Pressure at the last IC compressor outlet/at CO_2 delivery, bar	88/110
Pressure at the dehydration vessel, bar	15
Pressure drop in each intercooler, %	1
Pump hydraulic/mechanical efficiency, %	75/80

[6] The gas turbine model by Chiesa and Macchi [18] was used to simulate the advanced combustion turbine [27].

[7] It is worth underlining that the H_2S to CO_2 ratio in the gas entering the AGR station is very low. Thus, in the H_2S removal section a diluted MDEA solution was considered: it helps in increasing the liquid flow rate and in maintaining a low residence time, while satisfying the desired specifications, so that the column is suitable to treat the high gas flow rate with an acceptable liquid-to-gas ratio and the selectivity towards H_2S is increased.

Table A.4. Main overall results for the IGCC plants with no CO_2 capture[8]

	L10	*L20*	*L30*
Cold gas efficiency, %	75.1	72.4	68.9
Net electric power, MW_{el}	920.14	950.87	985.68
Net electric HHV efficiency, %	46.26	45.21	43.47
Net electric LHV_{AR} efficiency, %	58.91	57.57	55.35
Net electric LHV_{AD} efficiency, %	48.70	48.26	47.25
Specific emissions, kg_{CO2}/MWh	731.10	745.80	772.50

Nomenclature

AGR	acid gas removal
AD, AR	after drying, as received
C&S	capture and storage
CT	combustion turbine
ER	CO_2 emission rate, kg_{CO2}/kWh
HHV, LHV	higher, lower heating value, MJ/kg
HP/MP	high/medium pressure, bar
HR	heat rate, kJ/kWh
HT/LT	high/low temperature, °C
IC	intercooled
IGCC	integrated gasification combined cycle
$\dot{m}$	mass flow rate, kg/s
MDEA	methyldiethanolamine
NRTL	Non-Random Two-Liquid
ref	reference (power plant with no CO_2 capture)
SPECCA	specific primary energy consumption for CO_2 avoided, MJ/kg_{CO2}
WGS	water-gas shift
WTA	Wirbelschicht Trocknung mit interner Abwärmenutzung
ΔT	temperature difference, °C
η	efficiency

References

[1] Giuffrida A., Romano M.C., Lozza G., Thermodynamic analysis of air-blown gasification for IGCC applications. Applied Energy 2011;88(11):3949-3958.

[2] Ishibashi Y., Shinada O., First year operation results of CCP's Nakoso 250MW air-blown IGCC demonstration plant. In: Gasification Technologies Conference 2008, Washington, DC, USA.

[3] Hashimoto T., Sakamoto K., Kitagawa Y., Hyakutake Y., Setani N., Development of IGCC commercial plant with air-blown gasifier. Mitsubishi Heavy Industries Technical Review 2009;46(2):1-5.

[4] Giuffrida A., Romano M.C., Lozza G., Efficiency enhancement in IGCC power plants with air-blown gasification and hot gas clean-up. Energy 2013;53:221-229.

[5] Giuffrida A., Bonalumi D., Lozza G., Amine-based post-combustion CO_2 capture in air-blown IGCC systems with cold and hot gas clean-up. Applied Energy 2013;10:44-54.

[6] Bonalumi D., Giuffrida A., Lozza G., A study of CO_2 capture in advanced IGCC systems by ammonia scrubbing. Energy Procedia 2014;45:663-670.

[7] Moioli S., Giuffrida A., Gamba S., Romano M.C., Pellegrini L., Lozza G., Pre-combustion CO_2 capture by MDEA process in IGCC based on air-blown gasification. Energy Procedia 2014;63:2045-53.

[8] Slight differences with respect to the results in [10] are due to the assumptions for the combustion turbine calculations.

[8] Bhattacharya S., Tsutsumi A., An overview of advanced power generation technologies using brown coal. In: Li C.Z., editor. Advances in the science of Victorian brown coal. Oxford: Elsevier. 2004. p. 360-400 [chapter 7].

[9] Hashimoto T., Sakamoto K., Yamaguchi Y., Oura K., Arima K., Suzuki T., Overview of integrated coal gasification combined-cycle technology using low-rank coal. Mitsubishi Heavy Industries Technical Review 2011;48(3):19-23.

[10] Giuffrida A., Impact of Low-Rank Coal on Air-Blown IGCC Performance. In: Proceedings of ASME Turbo Expo 2014; 2014 June 16-20; Düsseldorf, Germany.

[11] Karthikeyan M., Zhonghua W., Mujumdar A.S., Low-rank coal drying technologies - Current status and new developments. Drying Technology 2009;27(3):403-415.

[12] Osman, H., Jangam, S.V., Lease, J.D., Mujumdar, A.S., Drying of low-rank coal (LRC)- A review of recent patents and innovations. Drying Technology 2011;29(15):1763-1783.

[13] Kakaras E., Ahladas P., Syrmopoulos S., Computer simulation studies for the integration of an external dryer into a Greek lignite-fired power plant. Fuel 2002;81(5):583-593.

[14] Zuideveld P.L., Shell coal gasification process using low rank coal. In: Gasification Technologies Conference 2005, San Francisco, CA, USA.

[15] Aziz M., Kansha Y., Kishimoto A., Kotani Y., Liu Y., Tsutsumi A., Advanced energy saving in low rank coal drying based on self-heat recuperation technology. Fuel Processing Technology 2012;104:16-22.

[16] Giuffrida A., Romano M.C., Lozza G., CO_2 capture from air-blown gasification-based combined cycles. In: Proceedings of ASME Turbo Expo 2012; 2012 June 11-15; Copenhagen, Denmark.

[17] GS (Gas-Steam cycles) - Available at: http://www.gecos.polimi.it/software/gs.php [accessed 30.12.2014].

[18] Chiesa P., Macchi E., A thermodynamic analysis of different options to break 60% electric efficiency in combined cycle power plants. Journal of Engineering for Gas Turbine and Power 2004;126(4):770-785.

[19] Giuffrida A., Romano M.C., Lozza G., Thermodynamic assessment of IGCC power plants with hot fuel gas desulfurization. Applied Energy 2010;87(11):3374-3383.

[20] Giuffrida A., Romano M.C., On the effects of syngas clean-up temperature in IGCCs. In: Proceedings of ASME Turbo Expo 2010; 2010 June 14-18; Glasgow, UK.

[21] Langé S., Pellegrini L.A., Moioli S., Picutti B., Vergani P., Influence of Gas Impurities on Thermodynamics of Amine Solutions. 1. Aromatics. Ind Eng Chem Res 2013;52(5):2018-2024.

[22] Pellegrini L.A., Langé S., Moioli S., Picutti B., Vergani P., Influence of Gas Impurities on Thermodynamics of Amine Solutions. 2. Mercaptans. Ind Eng Chem Res 2013;52(5):2025-2031.

[23] Astarita G., Savage D.W., Bisio A., Gas Treating with Chemical Solvents. New York, USA: Wiley; 1983.

[24] Moioli S., Pellegrini L.A., Gamba S., Li B., Improved rate-based modeling of carbon dioxide absorption with aqueous monoethanolamine solution. Front Chem Sci Eng 2014; 8(1):123-131.

[25] Moioli S., Pellegrini L.A., Improved rate-based modeling of the process of CO_2 capture with PZ solution. Chem Eng Res Des 2015; 93:611-620.

[26] Moioli S., Pellegrini L.A., Picutti B., Vergani P., Improved rate-based modeling of H_2S and CO_2 removal by MDEA scrubbing. Ind Eng Chem Res 2013;52(5):2056-2065.

[27] European best practice guidelines for assessment of CO_2 capture technologies - Available at: http://caesar.ecn.nl/fileadmin/caesar/user/documents/D_4.9_best_practice_guide.pdf [accessed 30.12.2014].